



## Surface integrity of hard alloys after machining using PCBN

H. Berns, K. Segtrop, W. Theisen

*Lehrstuhl Werkstofftechnik, Ruhr - Universität  
Bochum, 4630 Bochum, Germany*

### ABSTRACT

Turning tests on Co- and Fe- Base hardfacing alloys brought about that even hyper- and hypoeutectic alloys can be machined using CBN as the tool material. The flank wear of the cutting tool is mainly governed by the cutting speed and feed rate showing a minimum at a certain value.

The most important factors for the state of the surface and the subsurface are the cutting temperature (generated the cutting process) and the constituents of microstructure. At high temperatures carbides are plastically deformed while at lower temperatures a decohesion between the carbides and the matrix is found.

The quality of of a turned surface is comparable to a ground one, if optimal cutting parameters are choosen.

### INTRODUCTION

The quality of a machined surface is becoming more and more important to satisfy the increasing demands of industry /1/. In response the needs of more resistance against corrosion and wear there has been a continued increase in the development and use of hardfacing alloys /2/. Hardfacing alloys are deposited on tools and machine components by welding and thermal spraying. In many cases the resulting rough surface has to be machined by finishing operations. In the past these alloys could only be machined by grinding. Due to the development of new tool materials (polycrystalline cubic boron nitride, PCBN ; polycrystalline diamond, PCD) it has become possible to turn hardfacing alloys instead of grinding them. It is known from high strength

materials, that surface effects produced by machining may have a significant influence on the material properties. These effects are depending on the machining parameters such as cutting speed, feed rate and tool geometry as well as on the work,- and tool material /3-5/. The changes in the surface dictate that increased attention must be paid to possible failures by wear, fatigue and stress corrosion cracking. Such failures start at the surface of a component and depend very sensitively on the surface and the subsurface /6/. Most of the previous work dealt with the machined surface of single phase materials such as steels, Ni- and Co-Base superalloys. The microstructure of hardfacing alloys consists of hard phases (carbides and borides) which are embedded in a metal matrix of Fe,- Ni or Co- base. The amount, distribution and hardness of the hard phases is mainly responsible for wear resistance in practical applications /7/.

The aim of the present investigations is to find out which cutting parameters lead to a minimum of tool wear and surface damage. Furthermore the surface analysis gives knowledge of the cutting mechanisms in multiphase hard alloys which enables one to choose the optimal cutting parameters.

## EXPERIMENTAL WORK

Cutting tests were carried out on two Co- base and two Fe- base alloys. The Co- base Stellite 6 was deposited on steel shafts of 90 mm diameter and 500 mm length using open arc welding or the powder metallurgical HIP method (hot isostatical pressing). The chemical composition is given in Table 1.

Alloy	Co	Cr	W	Si	Ni	Fe	C	Hardness (HRC)
Stel.6 W	bal.	28	4,5	0,9	0,8	4,3	1,3	45-49
Stel.6 PM	bal.	28	5,0	1,3	--	3,0	1,3	48-50

**Table1: Chemical composition of the layers in weighth-%**

**Figure 1** shows the microstructure of Stellite 6 in the as welded (W) and as hipped condition (PM). In the as welded condition a netlike structure of eutectic  $M_7C_3$  carbides surrounds the metal cells of about 20  $\mu\text{m}$  diameter. The PM- layer shows a fine dispersion of globular carbides of the same type in the same solid solution strength and metal matrix.

The Fe- base alloys were manufactured as castings of 120 mm diameter. Due to the lower rate of solidification their eutectic net is coarser than that of the Co- base weld deposit. The chemical composition of the investigated Fe- Base alloys is given in Table 2.

Alloy	C	Cr	Mn	Nb	Si	Mo	Ti	Hardness (HRC)
X210	1,9	11,3	0,36	--	0,34	0,27	--	62
X230	2,3	12,8	0,45	8,5	0,97	0,79	0,45	61

**Table 2: Chemical composition of the Fe- Base alloy in weighth-%**

Figure 2 shows the microstructure of X 210 Cr and X 230 with the same netlike structure of eutectic carbides surrounding metal cells as in Stellite 6 W. The X 230 shows 15 vol%. of primary NbC carbides beside the eutectic  $M_7C_3$ - carbides, which are much harder than the  $M_7C_3$ - carbides. The metal cells consist of a Fe-Cr-C solid solution.

The cutting tests were carried out on a universal cutting machine under dry conditions using PCBN as the tool material with a rake angle of  $-8^\circ$ . The cutting forces were recorded with a piezoelectric threecomponent cutting force dynamometer while the process temperature was measured by infrared thermometer. The hot turning test were done with the help of a plasma arc heating up the workpiece 70 mm in front of the tool. The flank wear of the tool material ( $V_B$  and  $V_{Bmax}$ ) were determined using optical and scanning electron microscopy (SEM). A profilometer was used to measure the surface roughness. For the analysis of the surface and the subsurface, radial sections were ground on SiC abrasive paper of 1000 mesh size and afterwards polished and etched. The microstructure was investigated by SEM. The hardness measurements were done using the Vickers- method under a load of 294.2 N or 0.1- 0.49 N.

## RESULTS AND DISCUSSION

### TOOL WEAR

The cutting tests lead to two different trends in wear. Figure 3 shows the flank wear versus the cutting speed for Stellite 6 W after 5 minutes of conventional and 5 minutes hot machining (6 kW plasma power). For conventional machining it can be seen, that there is a minimum in tool wear



at 90 m/min. Higher and lower cutting speeds lead to an increase in flank wear and cutting forces.

There is a difference in the appearance of wear at high and low cutting speeds. At low cutting speeds notches occur at the end and the beginning of the cutting edge leading to high  $V_{Bmax}$  values. This can be explained by build up edges which are formed at low cutting speeds and then transported over the top face. There is no build up edge formation at higher cutting speeds so that the flank wear above the optimal cutting speed is much more even without extreme notches. After heating up the work material by plasma arc a different run of the wear curve versus the cutting speed was found. The right part of the graph (increasing flank wear at higher cutting speed) is shifted to lower cutting speeds.

If additional heat is brought in from outside by a plasma arc ahead of the tool, the characteristic temperature for the disappearance of build up edges is lowered and by this the flank wear, too. Additionally the plasma arc leads to a reduction in the strength of the workpiece material, so that plastic deformation and material decohesion occur at lower strength levels. This can be seen in **Figure 4** where the cutting forces are plotted versus the cutting speed for conventional and hot machining. For two feed rates the cutting force  $F_c$  is significantly lower in hot machining /8/.

Stellite 6 PM was produced to determine the influence of size and distribution of hard phases on the wear behaviour of the tool material. First results show a lower flank wear as compared to the weld deposits (**Figure 4**). The dispersion of the smaller hard phases leads to better deformability of the work material than a netlike structure. This results in a lower mechanical load at the cutting edge bringing about smaller scratches on the tool material surface.

In **Figure 5** the flank wear of CBN cutting tools after 5 minutes testing time is illustrated versus the cutting speed for the as cast Fe- Base alloys. The alloy X 210 shows no minimum in flank wear, but a continuous increase with rising speed. This can be explained by the build up edge formation. The surface analysis of the cutting tool after machining X 210 with extremely low cutting speed ( $v_c = 30$  m/min) revealed small areas of build up edge formation. This cutting speed is possibly a minimum in flank wear if additional test with lower cutting speeds would be carried out. For the Fe- Base alloys the flank wear obviously depends on the volume fraction and the properties of the hard phases and the acting temperature. This is confirmed by the wear results of X 230 which has the same microhardness in the metal matrix as alloy X 210 but additional primary hard phases of the NbC type.

## SURFACE INTEGRITY

The mechanism of chip formation is of great importance for the creation of the new surface. **Figure 6** shows a schematic drawing of chip formation together with a section through a quick-stop specimen. The edge of the tool penetrates into the work piece which is elastically and plastically deformed. A chip is formed by shearing the work material in the primary shear zone (1) and moving it over the rake face of the tool. For the formation of the new surface the secondary shear zone (3) is of great interest /9/. Frictional sliding between tool and work material introduces shear strains and plastic deformation under the newly generated surface. There is a region of extremely high plastic strain on the contacting side of the chip /10/. This area at the interface of rake face and work material is called flow zone (4). Due to the seizure at this interface and because of the extreme intensity of strain in the flow zone the temperature is much higher than in the body of the chip. In this region no cracks can be observed, but on the distinctly colder free side the chip is splitted by microcracks. The thickness of the influenced zones mainly depends on the cutting parameters and the work material. This can be confirmed by investigating sections through the machined surface. **Figure 7** shows that the network of eutectic carbides is destructed in the surface near zone up to a depth of about 10  $\mu\text{m}$ . Depending on the cutting parameters there are two different destructing mechanisms:

At a cutting speed of 90 m/min and a feed rate of 0.312 mm/rev the metal cells as well as the eutectic carbides are plastically deformed without any crack formation, due to high process temperatures.

(**Figure 7a**)

At a cutting speed of 65 m/min and a feed rate of 0.1 mm/rev the process temperature is much lower. In this case only the metal cells are plastically deformed by the mechanical load. In contract to the mechanism described above, the carbides cannot be deformed at this process temperatures, which leads to a decohesion between them and the metal matrix. (**Figure 7b**)

Considering the results above, the temperature is the most important parameter for tool wear and surface integrity /11/.

Beside the visual changes in the surface and the surface near zone of the work material there are changes in the microhardness. **Figure 8** shows the microhardness of the workmaterial as a function of the distance from the surface after machining with different cutting speeds and a feed rate of 0,312 mm/rev. The hardness in the surface is much higher than in the bulk material.

This can be explained with the help of transmission electron microscopy (**Figure 9**). 6  $\mu\text{m}$  below the surface a high density of stacking faults are found, which indicates that work hardening must have taken place in this zone. With increasing distance from the surface the density of the stacking faults becomes smaller leading to a decrease of hardness (**Figure 7**).

The comparison of the three different cutting speeds shows an equal profile of the curves at 65 m/min and 180 m/min (**Figure 8**). A distinctly smaller increase and a lower depth of influence is to be observed at a cutting speed of 90 m/min. This correlates with the results of tool wear in **Figure 3**.

An investigation of the Fe- base alloys shows the same destruction of the eutectic net- like structure as can be seen in **Figure 5** for Stellite 6 W, but no changes in microhardness are found. Due to the lower work hardening capability and higher rate of thermal softening of the bcc Fe- matrix there is no difference between the hardness of the surface and the bulk material.

## SURFACE TOPOGRAPHIE

Beside the machining parameters the wear of the cutting tool discribed above is responsible for the type of surface. A relatively low cutting speed leads to a relatively rough surface ( $R_z = 3,5 - 7 \mu\text{m}$ ). At higher cutting speeds the surface quality is improved, although the wear rates increase ( $R_z = 2-3 \mu\text{m}$ ). A higher cutting speed produces a higher process temperature and the resistance of the work material against deformation is reduced. **Figure 10** shows that for cutting speeds  $v_c \leq 90$  m/min the surface quality of a hot machined specimen is much better (conventional  $R_z = 3-7 \mu\text{m}$  / hot machined  $R_z = 1-3 \mu\text{m}$ ), because of the additional energy which is brought into the process by heating.

By choosing the optimal cutting speed the surface quality achieved in conventional as well as hot machining is comparable to ground surfaces.

## CONCLUSIONS

Tool wear and surface integrity was investigated in cutting four Fe- and Co-Base alloys. This revealed the following:

The analysis of chip formation brought basic knowledge of the cutting mechanisms for alloys containing hard phases.

The important factors influencing the state of the surface as well as the tool wear are the cutting temperatures and the properties of the microstructure constituents.

The tool wear of alloy Stellite 6 W mainly depends on the cutting speed

showing a minimum, which is shifted to a lower cutting speed by hot machining.

Additional tests on the simulation of wear mechanisms effecting wear of the tool material and hot machining on Fe- Base alloys are under way.

#### ACKNOWLEDGEMENT

This investigation was sponsored by the Deutsche Forschungsgemeinschaft under contract SFB-315 B5 and C5. The authors like to thank Dipl.Ing D. Biermann and Dr.Ing. D.Meister for their support during this work.

#### 4. References

- /1/ M. Field, W. Koster, J. Kahles: "Effect of machining practice on the surface integrity on modern alloys" , Paper from the International Conference Manufacturing Technology, 1967 p. 1319-1336
- /2/ H.Uetz: "Abrasion und Erosion", Carl Hanser Verlag, Wien 1986 p.374-394
- /3/ M. Field, J.F. Kahles, W.P. Koster: "Surface Integrity in Machining and Grinding", Technical Paper of Society of Manufacturing Engineers, Dearborn, Michigan, No. MR 67-142 (1968)
- /4/ E. Brinksmeier: "Beeinflußung physikalische Werkstückeigenschaften durch spanende Bearbeitung", VDI-Z Bd.126 (1984) Nr.23/24, p.929-933
- /5/ H.K. Tönshoff, H. Trumhold, E. Brinksmeier, H.G. Wobker: "Surface Layers of Machined Ceramic", Annals of the CIRP Vol.38(1989)2, p.699-708
- /6/ J. Bailey, S. Jeelani: " Surface integrity in machining 18% Ni maraging steel", Technical Papers, American Society of Tool and Manufacturing Engineers, No. IQ. 74-185, 1974
- /7/ H. Berns: "Eisenwerkstoffe mit harten Phasen und erhöhtem Verschleißwiderstand". Stahl u. Eisen 105 (1985) 16, p. 813-817
- /8/ H. Berns, K. Weinert, D. Meister, W. Theisen: "Machining of Wear Resistant Thick Coatings", to be published in DGM- Conference Proceedings, "Surface Engineering", March 1993, Bremen
- /9/ G. Warnecke: "Spanbildung bei metallischen Werkstoffen", Fertigungstechnische Berichte, Band 2, Gräfling, Resch 1974
- /10/ E.M. Trent: "Metal Cutting and the Tribology of Seizure II, Movement of Work Material over the Tool in Metal Cutting", Wear 128 (1988) p.47-64
- /11/ D. Meister, W. Theisen: "Drehbearbeitung von Hartlegierungen und deren Einfluß auf die Oberflächenrandzone", Industrie Diamanten Rundschau 3/1990, p.143-148

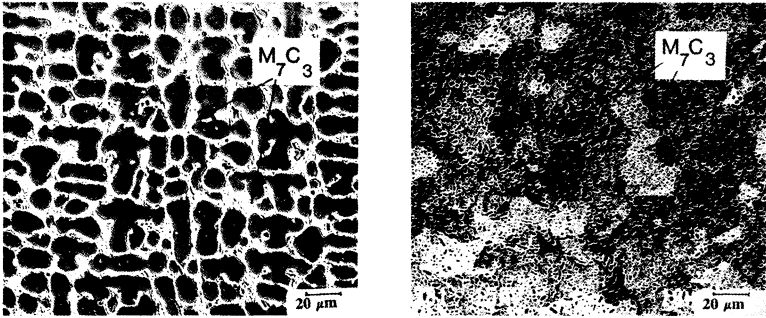
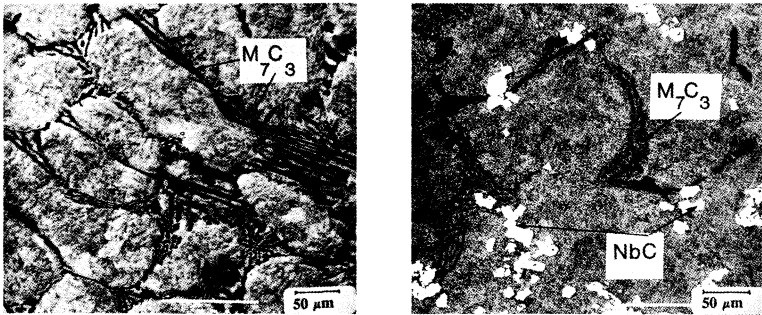


Figure 1: Microstructure of the Co- Base alloy Stellite 6



X 210

X 230

Figure 2: Microstructure of the Fe- Base alloys X 210 and X 230

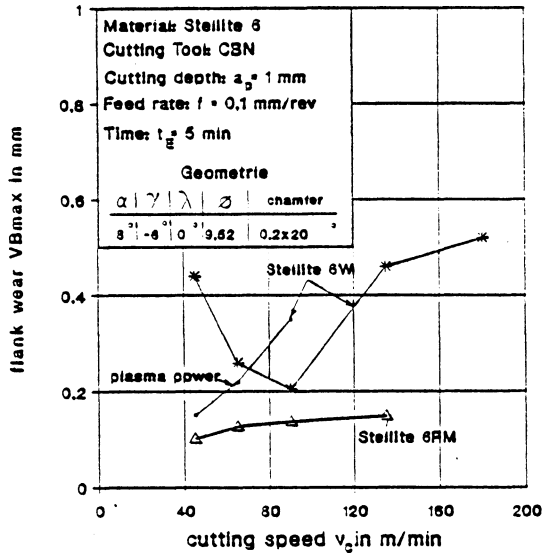


Figure 3: Flank wear versus cutting speed of the as cast Co- base alloys



### Surface Treatment Effects

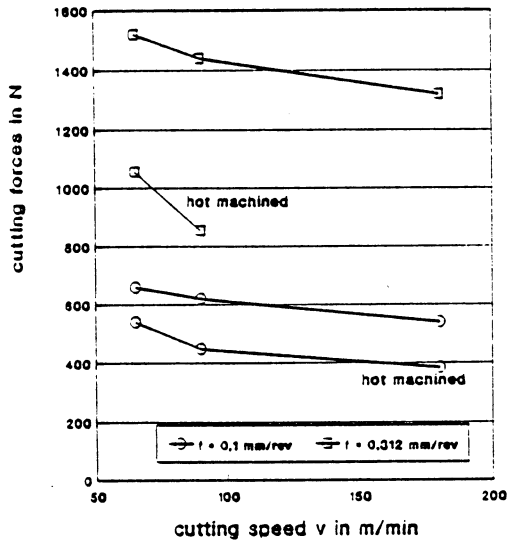


Figure 4: Cutting forces of conventional and hot machined Stellite 6 as welded  
X 210 / X 230

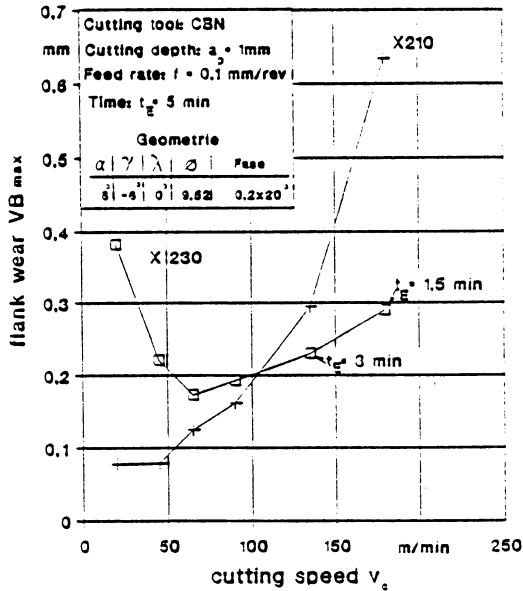
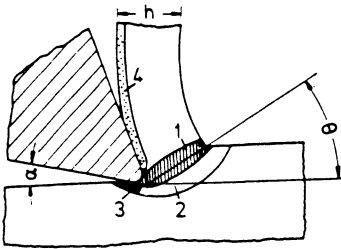
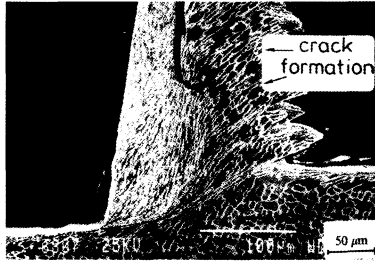


Figure 5: Flank wear versus cutting speed of as cast Fe- base alloys (X 210/X 230)



$\alpha$  = clearance angle  
 $\theta$  = shear angle  
 h = thickness of chip



1 : chip formation zone  
 2 : primary deformation zone  
 3,4 : secondary deformation zone

Figure 6: Chip formation (After Warnecke)

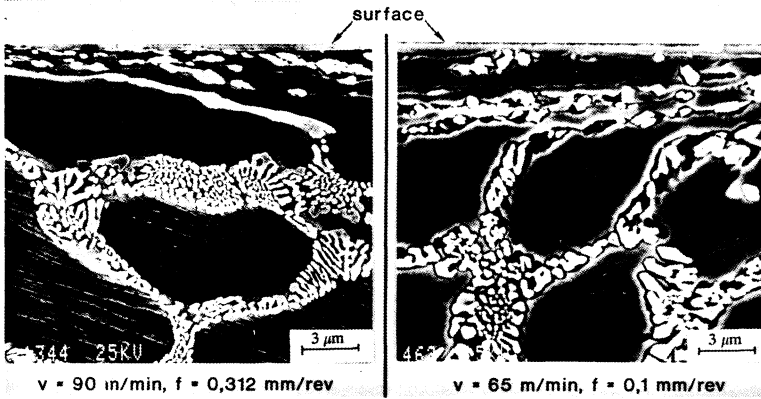


Figure 7: Destruction of the eutectic network in a surface near zone caused by machining

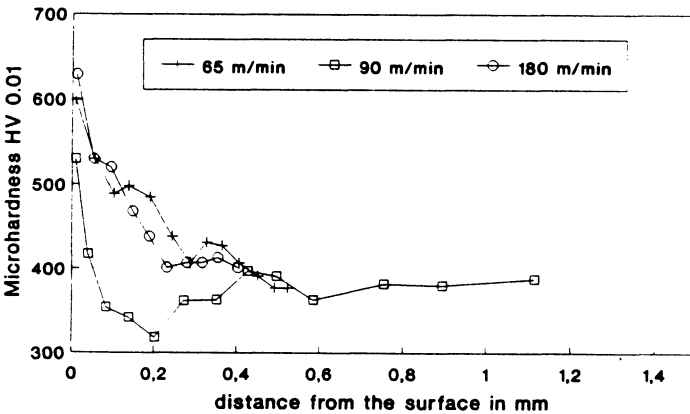


Figure 8: Microhardness of metal cells in Stellite 6 W after machining with PCBN

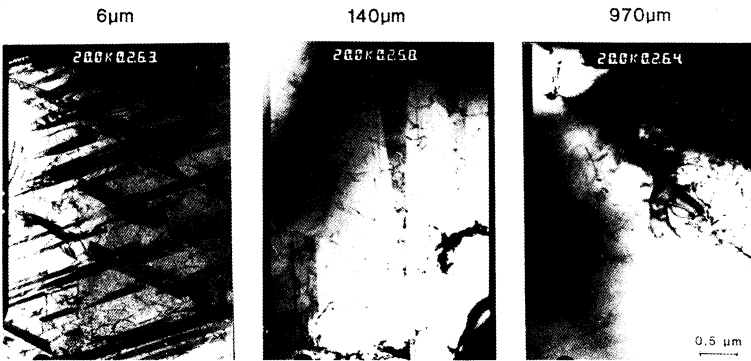


Figure 9: TEM- microstructure of Stellite 6 W under the machined surface

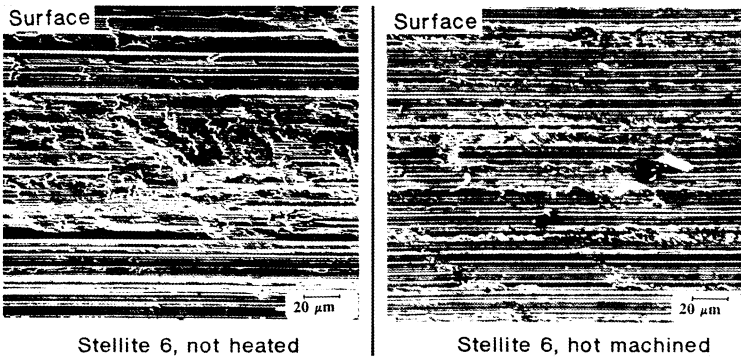


Figure 10: Machined surface of Stellite 6 W  
(cutting speed 65m/min / feed rate 0,1 mm/rev)